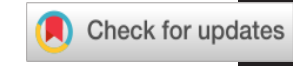
Prestack 3D and 4D seismic inversion for reservoir static and dynamic properties



Mosab Nasser¹, Dan Maguire¹, Henrik Juhl Hansen², and Christian Schiott¹

Abstract

We present a successful case study in which prestack 3D and 4D simultaneous AVO inversion is used in conjunction with rockphysics analysis to estimate saturation and pressure changes in a West Africa brownfield using time-lapse (4D) seismic as input. We show that, in 4D seismic, there can be many competing production effects that can be difficult to disentangle using traditional 4D interpretation methods, such as amplitude differences between the base and monitors. This begs the need for a more sophisticated approach to decouple these competing effects, such as the use of prestack simultaneous 3D and 4D inversions. Multiple substack seismic data are used to estimate a variety of 3D and 4D petroelastic attributes for mapping static and dynamic reservoir properties with the primary objective of influencing the continuous infill drilling and the overall reservoir management strategy. Facies-specific low-frequency models were used as priors for the 3D inversion, while velocity changes from time-lapse time shifts were used as priors for the 4D inversion. We also demonstrate the use of rockphysics templates coupled with a lithology-specific Gassmann fluid-substitution method to establish a nonlinear regression-based rock-physics model that obeys bound theory from classical rock physics and honors single and multimineral fluid-substitution theory. The resulting templates, when integrated with the prestack AVO-inversion technique, produce a set of attributes that accurately explain the time-lapse production effects observed on seismic.

Introduction

In brownfields, the need for effective reservoir monitoring becomes increasingly critical in the face of diminishing reserves and growing urgency for infill drilling and optimized recovery. Therefore, mapping reservoir saturation and pressure changes is vital for targeting bypassed hydrocarbons, evaluating well integrity, and drafting an overall reservoir management strategy. Such dynamic changes manifest themselves on both seismic amplitudes and lag time between events, which, when successfully interpreted, can lead to more informed decisions and better reservoir management. Reservoir depletion causes fluid expansion and an increase in effective stress, hence an increase in acoustic impedance is likely expected, unless gas comes out of solution to counter the increase in acoustic impedance. Similar changes in acoustic impedance are expected when water replaces hydrocarbons in a water-flood case, unless the sand is overpressured to override the saturation effects. Decoupling these competing time-lapse effects requires specific techniques, such as the use of time-lapse prestack inversion integrated with a rock-physics understanding.

We use prestack seismic inversion to analyze saturation and stress sensitivity of the reservoirs in the Okume complex, which contains five producing fields located in the Rio Muni Basin, located approximately 30 km offshore equatorial Guinea at a depth of about 2000 m true vertical depth subsea (TVDSS). The fields

were discovered in 2001 as submarine canyon systems that started during the Aptian and continued through and potentially beyond the Campanian period. These are typical West Africa deepwater turbidites, consisting of a series of confined and semiconfined vertically stacking and laterally migrating channel deposits. The primarily loose sands with clean sand porosities in the 30% range give rise to strong fluid effects, which in the case of the Okume complex means saturation effects will override pressure sensitivities in a coupled saturation-pressure 4D scenario. The Okume complex hydrocarbon-filled sands are of lower acoustic impedance and lower $V_{\rm P}/V_{\rm S}$ compared with the bounding nonreservoir shales, giving a class III AVO seismic response. However, aquifer sands are harder to map because of their transparent seismic response, similar to that of the bounding shales.

The primary objective of this study is to use a prestack seismic-inversion technology to invert for reservoir static and dynamic properties from 3D and 4D seismic data, for which rock physics is used to establish a link between the field's production and the observed time-lapse seismic effects.

The reason for the time-lapse prestack inversion is two-fold:

- Conversion from reflectivity to material properties as a part
 of the inversion process significantly improves the ability to
 interpret the often-complex amplitude changes observed in
 the Okume complex within the stacked and laterally varying
 channel deposits.
- The time-lapse signal (amplitude changes and time-lapse time shifts) is integrated with well-log data and converted to timelapse changes in elastic properties, which can be converted into changes in effective stress and fluid saturations using a rock-physics model.

Available data

The five fields contained within the Okume complex were discovered in 2001 on a standard 3D marine seismic survey acquired in 1999. However, in 2003, a WesternGeco 3D Q-marine data was acquired, forming the basis for full-field interpretation and development as well as a baseline for subsequent monitor surveys. Currently, more than 60 exploration, appraisal, and development wells are drilled in the Okume complex, some of which were used in the 3D and 4D prestack inversion for rockphysics calibration and seismic phase correction. Following the acquisition of the baseline in 2003, two subsequent high-repeatability monitor surveys were acquired in 2010 and 2014 with the WesternGeco Q-marine system. During acquisition of the two monitor surveys, two platforms were in place that were not present during the acquisition of the baseline survey in 2003. As a result, the two monitors have data gaps associated with the platform locations. The repeatability of the 2010 and 2014 monitor surveys

http://dx.doi.org/10.1190/tle35040415.1.

¹Hess Corporation.

²Qeye Labs ApS.

is high with the normalized rms of the time-lapse amplitude difference in areas of no production being 15%, thus making them suitable for monitoring the field's time-lapse saturation and pressure changes.

Seismic prestack depth-migrated gather data (baseline and monitors) and log data from a number of representative wells formed the input to the time-lapse prestack inversion. Figure 1 shows an example of a seismic line extracted from the baseline, monitors, and the 4D difference data.

Rock-physics analysis

Several wells from the Okume complex were analyzed to establish a nonlinear regression-based model (Westeng et al., 2009) that obeys bound theory from classical rock physics and honors single-Gassmann equation (Gassmann, 1951) and multimineral fluid-substitution theory. The rock-physics model connects the elastic moduli of the rock with porosity, mineral fractions, mineral moduli, and effective fluid moduli as presented in the following equations:

$$\frac{1}{K_{\text{mod}} + K_{\text{reg}}} = \frac{\varphi}{K_{\text{fluid}} + K_{\text{reg}}} + \frac{\left(1 - \varphi\right)V_{\text{clay}}}{K_{\text{clay}} + K_{\text{reg}}} + \frac{\left(1 - \varphi\right)\left(1 - V_{\text{clay}}\right)}{K_{\text{quartz}} + K_{\text{reg}}} \tag{1}$$

$$\frac{1}{G_{\text{mod}} + G_{\text{reg}}} = \frac{\varphi}{G_{\text{reg}}} + \frac{(1 - \varphi)V_{\text{clay}}}{G_{\text{clay}} + G_{\text{reg}}} + \frac{(1 - \varphi)(1 - V_{\text{clay}})}{G_{\text{quartz}} + G_{\text{reg}}}$$
(2),

where the modeled bulk and shear moduli, K_{mod} and G_{mod} , are related to the porosity, ϕ , the fluid bulk modulus, K_{fluid} , the bulk and shear mineral moduli for clay and quartz, K_{clay}, G_{clay} and K_{quartz}, G_{quartz} , and the bulk and shear regression terms, K_{reg} and G_{reg} .

Total porosity, clay content, and effective stress parameters were used to derive the regression parameters for the rock-physics model. Any variable that potentially influences the rock matrix can be used as a regression variable. The model is adaptable to any specific rock type and can be extended to include full anisotropy. Moreover, the model framework is flexible since it allows for calibration of the model to log data, capturing local trends of the Okume complex as well as honoring preferred theoretical models, e.g., those capturing pressure sensitivity.

All wells were fluid substituted using a Gassmann-consistent method by Nasser et al. (2013) suitable for depositional environments with thin bed response, as in the Okume complex, to avoid overestimation of the fluid response. The fluid-substituted logs were used to calibrate the magnitude of the fluid response expected from the rock-physics model and to form the basis for estimating the probability density functions for a Bayesian facies classification.

The purpose of the estimated rock-physics model for the Okume complex is three-fold:

- It serves as a forward model for modeling the elastic response of variations in mineral fractions, saturations, porosity, and
- It provides the framework for inverting absolute acoustic impedance, V_p/V_s , and density derived from seismic AVO data into mineral fractions, saturations, and porosity.

It provides the framework for inverting changes in acoustic impedance, $V_{\rm p}/V_{\rm s}$, and density estimated from time-lapse seismic AVO data into changes in saturations and effective stress.

Figure 2 shows the similarity between a set of crossplots of measured well-log data compared with crossplots of the elastic response from the globally estimated rock-physics model. It also shows the result of the laminated fluid-substitution modeling compared with the rock-physics-model-based fluid substitution showing similar magnitude of fluid response.

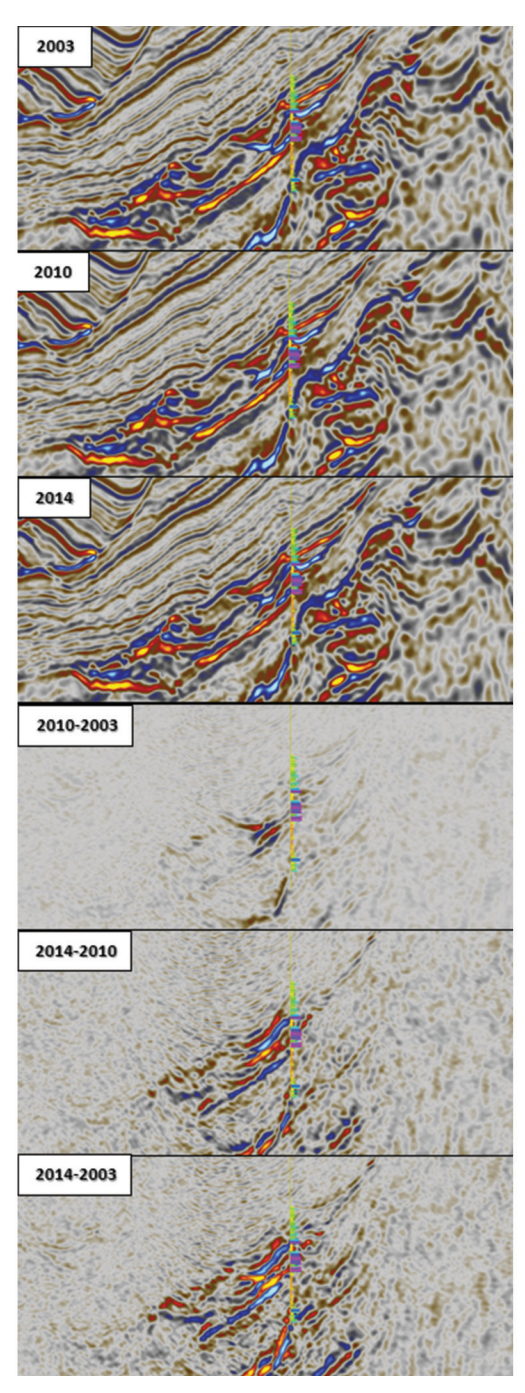


Figure 1. A seismic cross section across the Okume canyon from the full-stack data and associated amplitude differences for the three vintages: 2003, 2010, and 2014. Notice the high level of repeatability and the pronounced time-lapse amplitude signal.

3D and 4D simultaneous AVO-inversion workflow

A dedicated 3D prestack seismic inversion was conducted using preproduction 2003 preconditioned angle stacks. The seismic data was inverted for absolute acoustic impedance, $V_{\rm p}/V_{\rm S}$, and density using a 3D simultaneous AVO-inversion algorithm based on the Aki & Richards three-term reflectivity model. The 4D prestack inversion was based on a time-lapse simultaneous AVO-inversion algorithm also using the Aki & Richards three-term reflectivity model in which the multivintage prestack data are

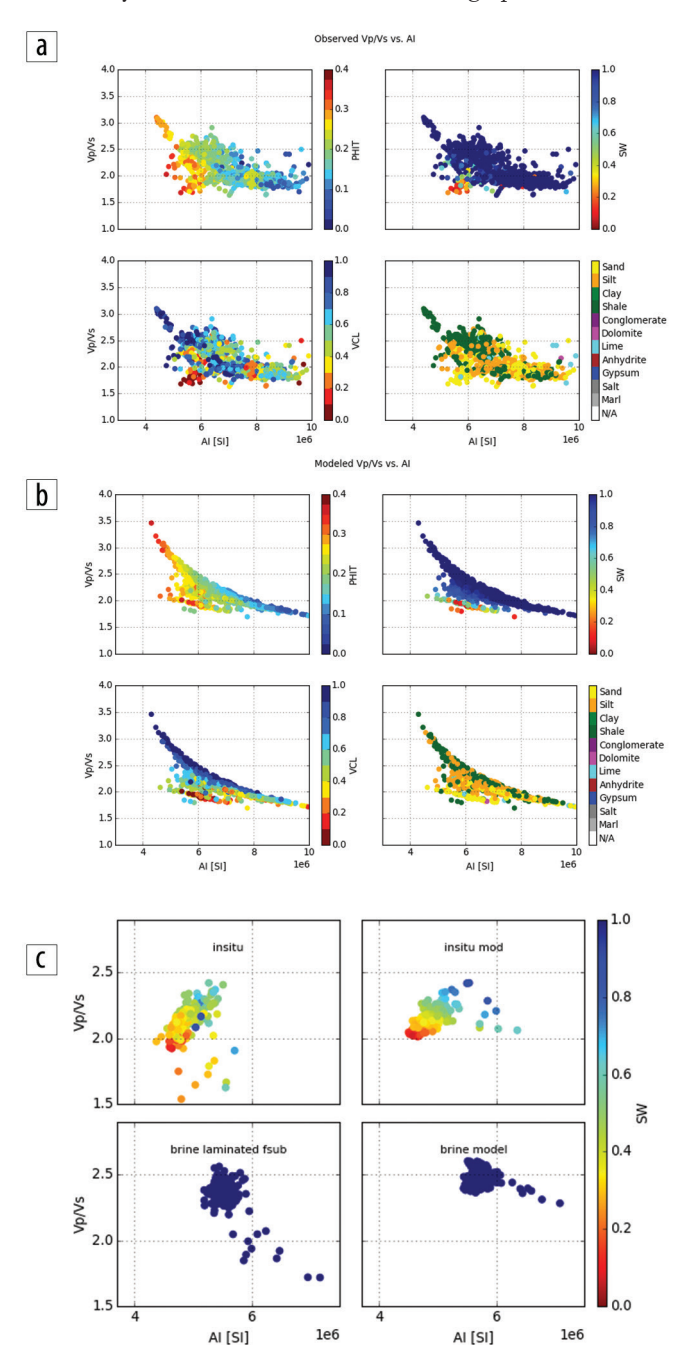


Figure 2. (a) Crossplots of measured well-log data color-coded with key reservoir properties compared with (b) crossplots of the elastic response of the globally estimated rock-physics model, which show a similar elastic response. (c) Laminated fluid substitution modeling compared with rock-physics model based fluid substitution showing similar magnitude of fluid response.

inverted directly for ratio changes in acoustic impedance, shear impedance, and density; each vintage is treated on an equal basis as shown in the following set of equations.

$$\begin{split} Z_1 &= Z_0 + \Delta Z_1 \\ Z_2 &= Z_0 + \Delta Z_2 \\ Z_3 &= Z_0 + \Delta Z_3 \\ \Delta Z_1 + \Delta Z_2 + \Delta Z_3 &= 0 \end{split} \tag{3}.$$

The logarithmic domain set of equations relates the impedances of three vintages, Z_n , to a mean model, Z_0 , via the differences. Note that the formulation is symmetrical with respect to any given vintage. For this reason, this symmetrical formulation ensures that, in a 4D sense, there is no notion of a baseline vintage.

The preconditioning of the seismic data involved the generation of a series of angle stacks with a 5° angle width from 0 to 60°. Each angle stack was subjected to frequency-dependent amplitude matching between vintages, zero-phasing using multiwell-based estimated wavelets, 4D, and angle domain warping/alignment relative to a reference stack selected from the preproduction data. Both time shifts and time strains were estimated between vintages. An optimal angle range for the inverted seismic data was found to be 10–50° despite the fact we had data available up to 60°. AVO-inversion tests demonstrated the added value of leaving out the 0–10° data primarily due to residual multiple energy and leaving out the 50–60° data due to the presence of refracted energy from high-velocity layers below the target interval.

Well ties of near-normal incidence data revealed some phase rotation of the seismic data, which was corrected. Statistical spectral analysis between the individual angle stacks revealed no phase rotation between them and was used to derive the zero-phase wavelets that were utilized in the inversion. Due to the vintage-to-vintage matching, including frequency-dependent amplitude balancing, the same wavelet was used for a specific angle range across each vintage.

A critical step for the prestack inversions was the building of facies-driven low-frequency models for acoustic impedance, $V_{\rm P}/V_{\rm S}$, and density, similar to Pillet et al. (2007). The objective is to extrapolate well-based facies-specific low-frequency trends out into the 3D volume and only use them for a facies where it is present. In this way, reservoir sand properties are not blindly extrapolated out into the entire 3D volume but only where reservoir sands are present.

For each of the facies — shale, sand (brine and oil), and cemented/poor sand — the low-frequency models were guided by the available seismic velocities and based on well-log data where only the relevant facies are present. Bayesian lithology classification using relative acoustic impedance and $V_{\rm p}/V_{\rm S}$ inversion results together with detrended well-log data were used to estimate 3D volumes of facies probabilities. These facies-probability volumes were used as weighting functions for building a set of hybrid low-frequency models for acoustic impedance, $V_{\rm p}/V_{\rm S}$, and density. The models were low-pass filtered to produce a weak-reflectivity low-frequency model for each property (acoustic impedance, $V_{\rm p}/V_{\rm S}$, and density) to minimize their bias on the inversion results. The validity of the approach was evaluated against well-log data.

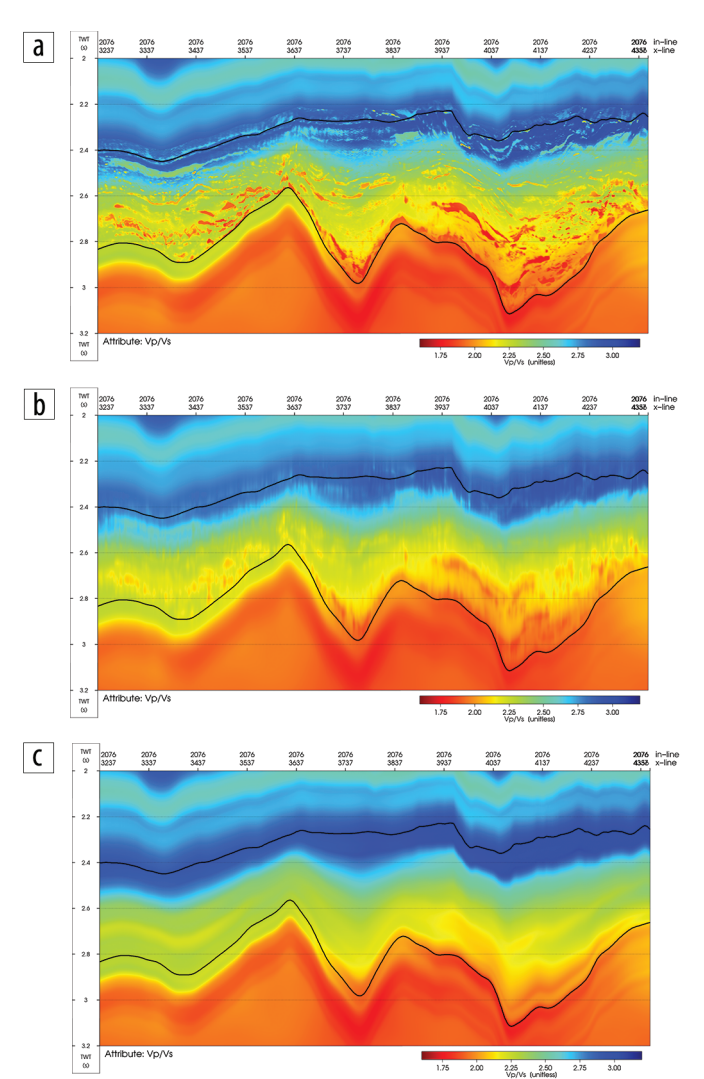


Figure 3. Cross sections of V_P/V_S low-frequency models. (a) Facies driven before low-pass filtering, (b) facies driven after low-pass filtering, and (c) a shale only low-frequency model.

Figure 3 shows a comparison between the facies-specific models (3a), the low-pass-filtered models (3b), and a shale-only model (3c), respectively. Figure 4 shows a comparison between the inverted acoustic impedance, $V_{\rm P}/V_{\rm S}$, and density against well data using the low-pass-filtered low-frequency models as input.

Another important step was building a set of 4D ratio change low-frequency models using the 4D relative changes in acoustic velocity derived from 4D time shifts under the (valid) assumption of a noncompacting reservoir. The change in acoustic velocity and its bias on changes in acoustic and shear impedance depends on the scale and type of production. For example, a replacement of fluid implies a change in acoustic velocity, whereas the shear impedance does not change significantly, as opposed to a decrease in effective stress, which almost equally impacts the changes in acoustic velocity and the shear impedance. This property- and production-dependent level of bias was inferred from spatially varying common-bandwidth cross-correlation volumes between the relative changes in velocity and relative 4D ratio changes in acoustic impedance and shear impedance from inversion results. The level of bias was calibrated to areas of known production, and the resulting models were low-pass filtered in order to retain only the frequencies below the seismic bandwidth.

The inverted relative changes in elastic properties only contain information within the seismic bandwidth with the changes in acoustic impedance, shear impedance, and the associated changes in $V_{\rm P}/V_{\rm S}$, demonstrating a strong correlation with production data. This correlation was even more pronounced for the inverted full-bandwidth changes in acoustic impedance and shear impedance, which use the 4D ratio change low-frequency models as prior information. This improved correlation with production data demonstrates, in the domain of changes in real physical properties, the consistency between information from 4D time shifts and 4D prestack amplitude information.

Figures 5 and 6 compare ratio changes in acoustic impedance and $V_{\rm p}/V_{\rm s}$, the low-frequency model, and relative and absolute inversion results. In this case, the top 4D anomaly is larger than

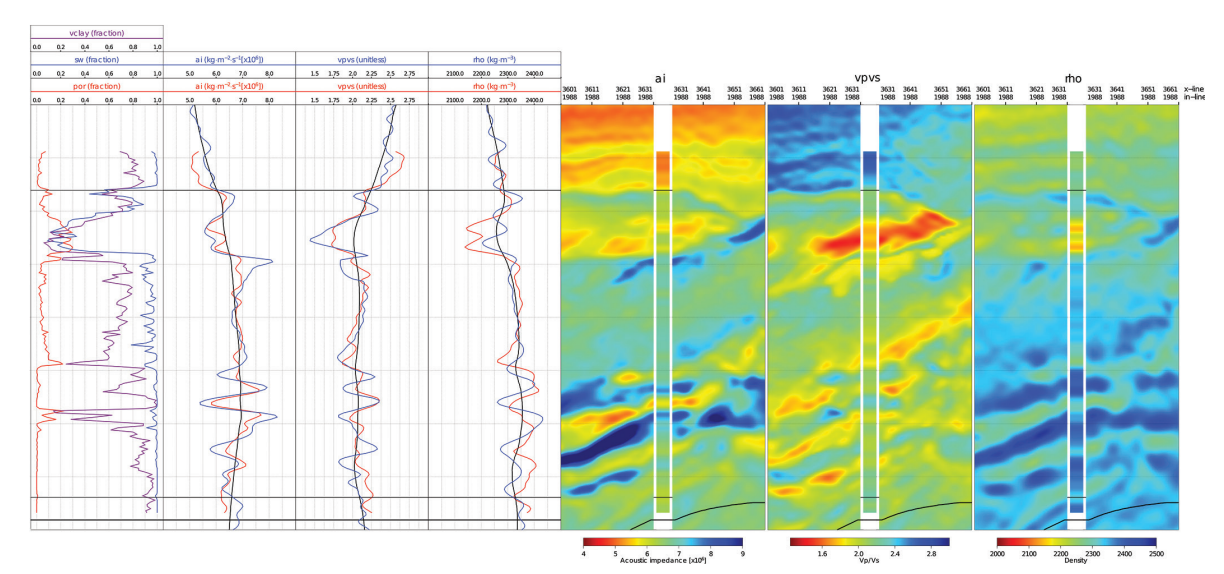


Figure 4. Absolute acoustic impedance, V_P/V_S and density inversion results for the 2003 vintage. From left to right: A set of petrophysical logs (volume of clay, water saturation, and porosity), inversion results in blue (AI, V_P/V_S , and density) compared with well-log data filtered to seismic bandwidth in red and the low-frequency model in black, and the well-log data are inserted into inverted sections around the well trajectory.

what has been predicted by the 3D facies probability. In many ways, one could argue that the 4D inversion should encourage one to make a larger sand region at the top, rather than masking it by the facies probability.

3D and 4D rock-physics-inversion workflow

The prestack seismic data was taken a step further. Using the available rock-physics models and well-log-data-based a priori correlations between total porosity, volume of clay, and water saturation, the baseline elastic products were inverted for preproduction water saturation, porosity, and volume of clay. For the 4D rock-physics inversion, and given that we are dealing with loose sands, a Hertz-Mindlin-like effective-stress formulation was used to account for changes in effective stress; see Smith et al. (2004) for more details. For the Okume complex, in the absence of any changes in fluid saturations, a pressure signal can be observed on seismic; however, in a coupled saturation-pressure

scenario, saturation effects will override the pressure effects due to the very high porosities of the sands. The full-bandwidth elastic 4D changes where inverted for changes in saturation and pressure. Figure 7 shows an excellent match between the rock-physics-based 3D and 4D inversion results and the petrophysical logs at one of the blind wells. A similar match was achieved at the remaining blind wells.

Analysis and discussion

Reservoir monitoring is a critical tool in field development and exploitation as a source of vital information on reservoir time-lapse changes related to production, such as saturation changes, drainage pattern, and stress changes. In the Okume complex, we see a wide range of 4D signals related to saturation changes, pressure depletion, and overpressure. Our ability to effectively interpret time-lapse seismic differences is influenced by our ability to decouple them into their individual components

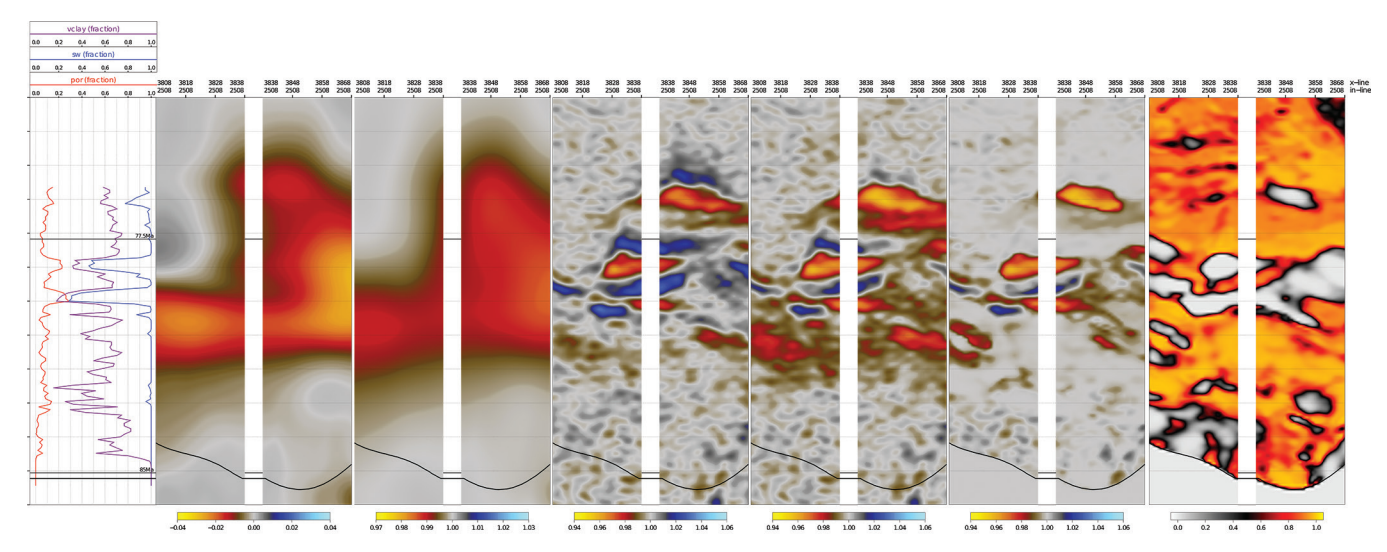


Figure 5. Change in acoustic impedance from 2003 to 2014 at a well location. From left to right: A set of petrophysical logs (volume of clay, water saturation, and porosity), relative change in acoustic velocity from 4D time shifts, 4D low-frequency model, relative change, absolute change, and absolute change masked to presence of reservoir using the facies probability of shale (far right).

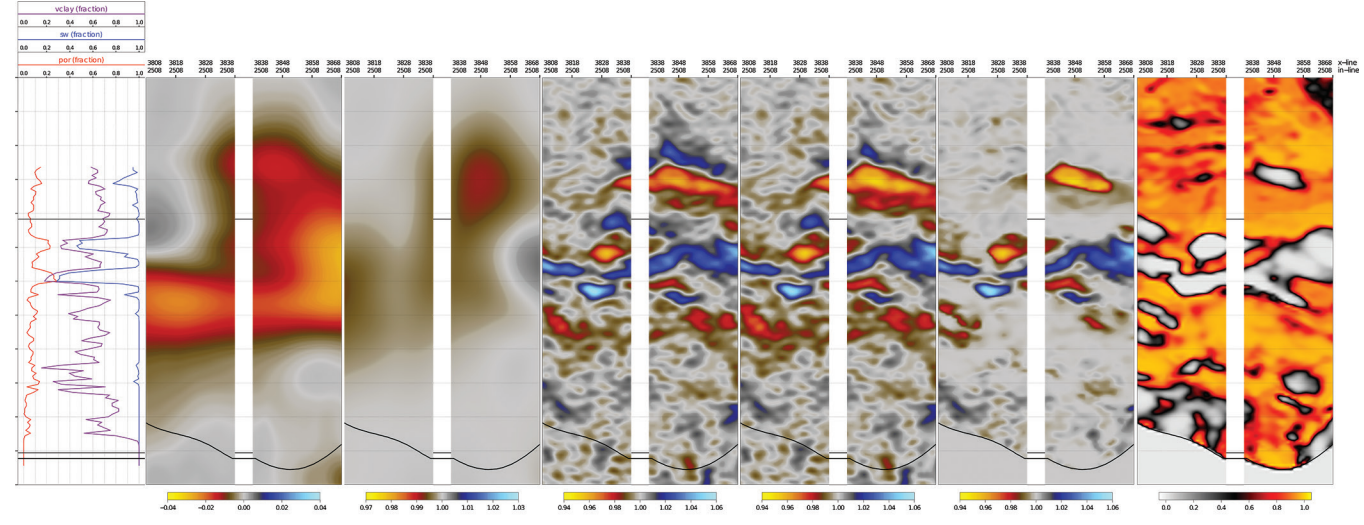


Figure 6. Change in V_p/V_s from 2003 to 2014 at a well location. From left to right: A set of petrophysical logs (volume of clay, water saturation, and porosity), relative change in acoustic velocity from 4D time shifts, 4D low-frequency model, relative change, absolute change, and absolute change masked to presence of reservoir using the facies probability of shale (far right).

Special Section: AVO inversion May 2016 THE LEADING EDGE 419

(saturation and pressure). Analysis of the inversion products, such as changes in acoustic impedance, shear impedance, and $V_{\rm P}/V_{\rm S}$, coupled with seismic attributes, such as angle substacks, intercept, gradient, time shifts, and time strains, have proven critical for identifying infill well-drilling opportunities and fluid-front movement.

To accurately interpret the 4D signal observed on seismic data, in Figure 8a and 8b we present two crossplots of AI versus $V_{\rm p}/V_{\rm s}$ and AI versus SI showing a series of possible scenarios generated using the 4D rock-physics model for different porosity groups and with varying pressures and saturations. This forms the basis for interpreting Figure 9, which shows a set of cross sections in an area near an active injector causing the reservoir pressure to increase by about 1000 psi, which highlights the need for integrating the different data types to decouple the changes seen on the time-lapse seismic data. At this location, the acoustic impedance (Figure 9e) is showing blue, indicating hardening "increase in acoustic impedance over time" for the good-quality sands in response to saturation changes (increase in water saturation) and red indicating softening "decrease in acoustic impedance over time" for the overpressured either poor-quality sands or high-quality unswept hydrocarbon sands. On the other hand, in Figure 9f, the shear impedance is showing softening (red) for both the good and poor-quality sands regardless of the fluid fill, indicating an overpressure signal. This

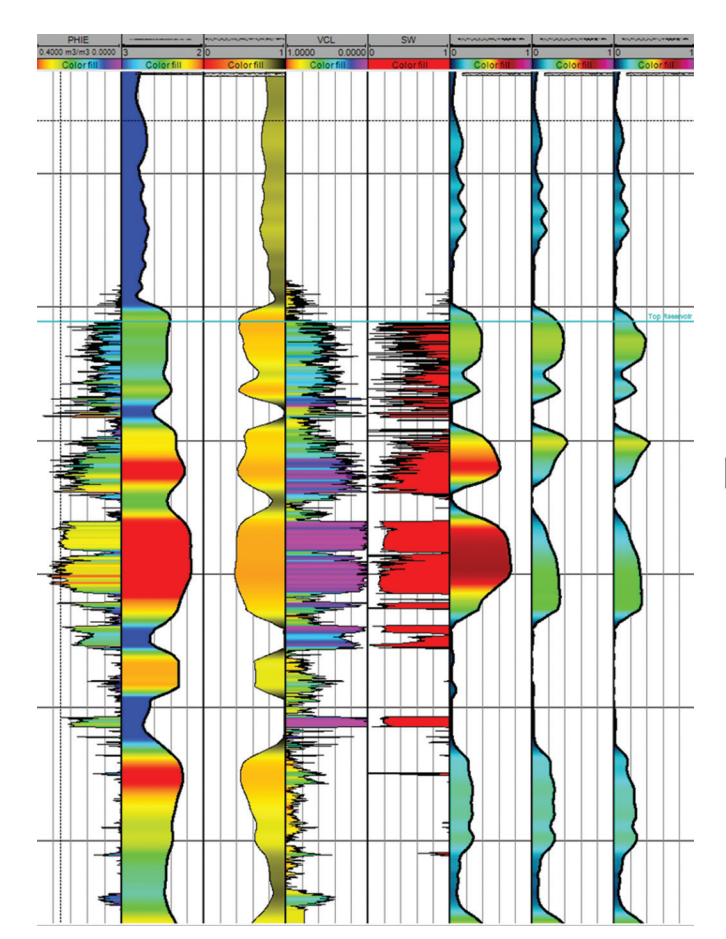
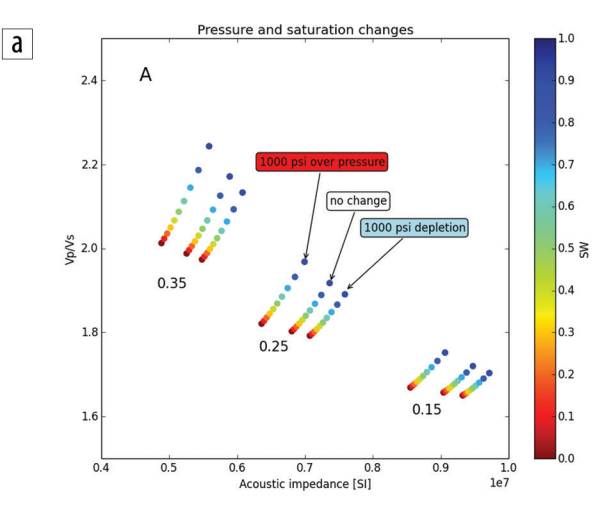


Figure 7. Inverted results compared against blind well data. Tracks from left to right: effective porosity, volume of clay, and oil saturations at 2003, 2010, and 2014. The well is located in an area of significant hydrocarbon production demonstrated by the last two tracks to the right.

means that, in the Okume complex, saturation effects override the pressure effects on the acoustic impedance change attribute, while, as expected, the shear impedance is relatively insensitive to fluid changes. This is a good example in which integration of different data attributes is critical for decoupling the competing production effects in the reservoir.

Conclusions

We have demonstrated that the use of 3D and 4D simultaneous seismic AVO inversions is critical for interpreting time-lapse changes in a brownfield environment to decouple competing production effects and achieve a comprehensive reservoir management strategy. Moreover, at the Okume complex, 3D and 4D inversion-based multiattribute analysis coupled with seismic data has proven successful in providing improved interpretation of the geology in addition to mapping saturation and pressure changes across the field for identifying infill drilling opportunities. The deliberate decision to build low-frequency facies-driven models has positively impacted the final 3D saturation, porosity, and volume of clay inversion results. Similarly, building 4D low-frequency models using



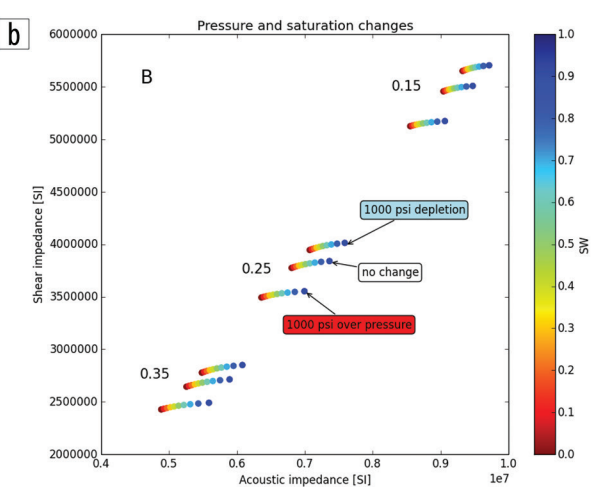


Figure 8. Scenario modeling of expected 4D changes based on the rock-physics model. The different lines represent the different porosity groups (0.15, 0.25, and 0.35) with varying pressures and saturations for each group.

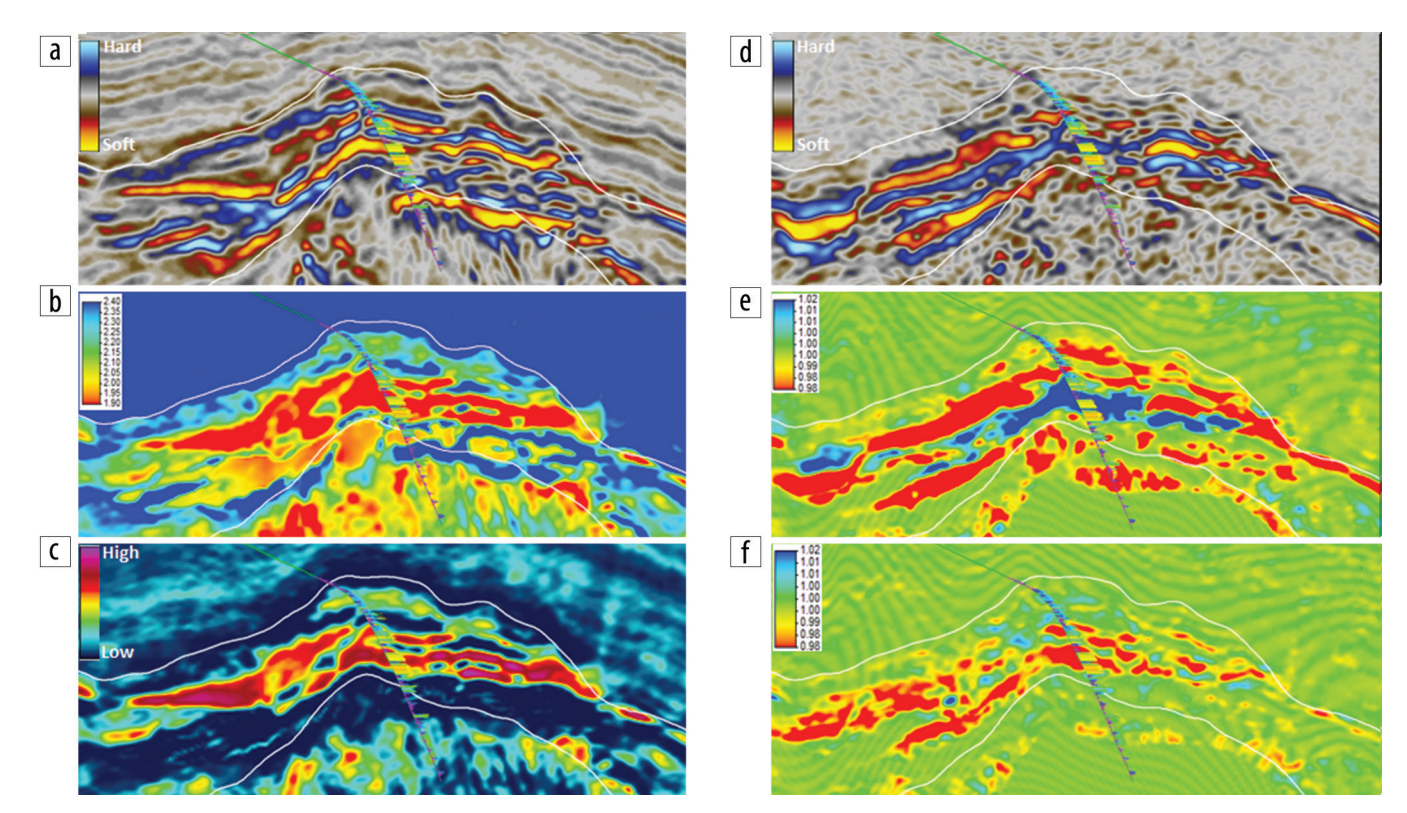


Figure 9. A set of cross sections showing how integration of different data types can be used to evaluate an area undergoing significant production. The different cross sections are: (a) 2003 full stack, (b) 2003 V_p/V_S ratio, (c) 2003 oil saturation, (d) full stack amplitude difference 2014–2003, (e) ratio change from 2003 to 2014 of acoustic impedance, and (f) shear impedance.

the 4D relative changes in velocity derived from time shifts to guide the estimation of the time-lapse changes in acoustic impedance and shear impedance has positively contributed to a more direct correlation between time-lapse seismic and production data. Finally, this study shows a successful use of the two-step approach to AVO inversion; that is, elastic inversion followed by rock-physics inversion. When the elastic 3D and 4D inversion results are derived from the seismic data and without relying on any rock physics, this makes them open to more exotic effects which are not accounted for in the rock-physics model, such as temperature change and shale swelling. The rock-physics inversion imposes a specific view of the rock properties via the rock-physics model onto the elastic results. Thus, the intermediate step serves as an excellent tool for quality control of the rock-physics model.

Acknowledgments

The authors would like to thank the Equatorial Guinean Ministry of Mines, Industry and Energy (MMIE), Hess Corporation, GE Petrol, and Tullow Oil for permission to publish this work. We would also like to thank many of our colleagues — in particular, Scott Marler, Chance Amos, J. P. Blangy, Vaughn

Ball, Michelle Thomas, and Robert Dunn — for their insightful comments and feedback throughout this work.

Corresponding author: mnasser@hess.com

References

Gassmann, F., 1951, Elastic waves through a packing of spheres: Geophysics, **16**, no. 4, 673–685, http://dx.doi.org/10.1190/1.1437718.

Nasser, M., I. Escobar, and H. Hansen, 2013, Rock physics evaluation of deepwater reservoirs, West Africa: 83rd Annual International Meeting, SEG, Expanded Abstracts 2407–2411, http://dx.doi.org/10.1190/segam2013-1261.1.

Pillet, W., E. Brechet, P. Mesdag, and M. Feroci, 2007, The quest for the low frequencies in prestack inversion: 77th Annual International Meeting, SEG, Expanded Abstracts, 1810–1814, http://dx.doi.org/10.1190/1.2792843.

Smith, B., D. Lane, and S. Danudjaja, 2004, Interpreting 4D seismic response to changes in effective pressure with rock physics modeling: Offshore Technology Conference.

Westeng, K., H. J. Hansen, and K. B. Rasmussen, 2009, A new petroelastic model for optimal rock physics inversion with examples form the Nini field: Sound of Geology Workshop.

Special Section: AVO inversion

422 THE LEADING EDGE May 2016